



Research on tribological behavior and mechanism of laser surface texturing on tool surface in hot stamping of Al-Si-coated high-strength steel

Mei Tangjie¹ · Zhang Qi¹ · Liu Xiaochuan¹ · Han Bin¹

Received: 18 October 2023 / Accepted: 30 April 2024 / Published online: 20 June 2024
© The Author(s), under exclusive licence to Springer-Verlag London Ltd., part of Springer Nature 2024

Abstract

The hot stamping of Al-Si-coated high-strength steel (HSS) sheets is an important manufacturing process that has gained significant attention in recent years. However, the friction and adhesive wear that occur during the process have become major bottlenecks, limiting the efficiency and effectiveness of the process. To address this problem, a comprehensive investigation was conducted to evaluate the tribological behavior of the contact interface between Al-Si-coated HSS sheets and tool steel during hot stamping. Specifically, micro-dimpled laser surface textures (LSTs) with varying densities were applied to the H13 tool steel surface, followed by an examination of their effectiveness in reducing friction and wear. The 3D morphology of the wear scratches was assessed using a laser confocal surface roughness system, while SEM and EDS techniques were utilized to analyze the mechanisms behind friction reduction and wear resistance. The results demonstrated that laser surface texturing (LST) effectively reduces the friction coefficient between Al-Si-coated HSS sheets and H13 tool steel under high-temperature and high-pressure conditions. Moreover, it was found that LSTs exhibiting densities of 30% retained their pitted morphology following friction experiments, indicating a remarkable capability in reducing adhesive wear and facilitating debris collection. The average coefficient of friction (COF) was observed to be significantly lower in textured specimens than in untextured specimens by approximately 64.62%, 52.3%, 51.9%, and 67.11% at pressures of 5 MPa, 10 MPa, 15 MPa, and 20 MPa, respectively. This study offers a novel concept and method that leverages the LST technology to mitigate the friction and wear of Al-Si-coated HSS sheets during the hot stamping process. The findings also shed light on the anti-wear effect and the mechanism of LST in such conditions. Overall, this study highlights the potential of LST as a promising method for enhancing the efficiency and effectiveness of the hot stamping process involving Al-Si-coated HSS sheets.

Keywords Adhesive wear · Laser surface texturing (LST) · Hot stamping process · Al-Si coating · High-strength steel (HSS) sheet

1 Introduction

High-strength steels (HSS) have been extensively used in the automotive industry, especially in the production of new energy vehicles due to their remarkable properties such as low cost, high toughness, specific strength and yield ratio, great weldability and formability, excellent machinability, and recyclability [1]. Among the various manufacturing

technologies used to form HSS sheets into complex-shaped components, the hot stamping process has emerged as a leading technology due to its ability to produce parts with low spring-back [2]. However, the hot-stamped uncoated sheet assemblies require an additional shot peening step to remove the oxide layer formed on their surfaces at high temperatures, which can significantly impact the surface quality of the component for subsequent treatments such as painting.

To overcome this issue and improve process efficiency, researchers have developed an Al-Si-coating that can be applied on HSS sheets. This coating is widely used due to its excellent weldability, spraying properties, and anti-depreciation protection, which eliminates the need for an additional shot peening process to remove the oxide

✉ Zhang Qi
henryzhang@xjtu.edu.cn

¹ School of Mechanical Engineering, Xi'an Jiaotong University, Xi'an 710049, Shaanxi, China

coating layer. However, during the hot stamping process of HSS under extreme operating conditions such as high temperature and loading pressure, the contact surface of the tool and sheet exhibit severe wear due to the transfer and accumulation of the Al-Si coating on the tool surface. This accumulation deteriorates the quality of the formed parts, leading to frequent tool refurbishment. Guo et al. [3] studied the high-temperature friction and wear conditions of the Al-Si coated and uncoated HSS sheets, and found that the Al-Si coating wore the tool surface more severely and the coefficient of friction (COF) was higher due to the hard intermetallic phases formed by the Al-Si coating interacting with Fe of the tool steel matrix. Despite these efforts, a comprehensive analysis to explain the friction and wear mechanism in hot stamping is yet to be conducted. Friction and wear remain one of the critical bottlenecks in the hot stamping process of HSS sheets [4]. Therefore, further studies are required to better understand the tribological behavior of HSS with Al-Si coatings during hot stamping and to develop effective solutions to reduce friction and wear, and improve the quality of the formed parts.

In previous studies, researchers have focused on reducing friction and wear on HSS with Al-Si coating during hot stamping. C. Boher [4] studied the wear behavior of US1-BOR1500P sheets under high-temperature conditions and identified adhesive wear as the main friction mechanism, with abrasive wear as the secondary friction mechanism. Ghiotti, A [5, 6] experimentally studied the tribological properties of Al-Si and Zn-based coatings on 22MnB5 sheets, and found that the COF of zinc-coated HSS sheet was low. The friction mechanism of the two coatings was identified to be a combination of adhesion and abrasive wear mechanisms. Azushima, A [7] studied the high-temperature friction behavior between an Al-Si coated 22MnB5 sheet and tools with different surface roughness, and discovered that the COF under dry friction conditions had a negligible relationship with the tool surface roughness. In addition, the friction force between the interface of the tool and the sheet was found to be mainly produced by the friction force between the thick adhesive materials on the tool surface and the Al-Si coating. Mu Y. H [2] studied the evolution of the Al-Si coating on the HSS sheet and its tribological properties at different elevated temperatures. The results showed that the COF decreased with increasing temperature of HSS sheets. At low temperatures, adhesive wear was identified to

be the dominant mechanism, while abrasive wear played a major role at high temperatures. Schwingenschl P [8] analyzed the friction and wear behavior at different temperatures, relative sliding speeds, and contact pressures. The results indicated that a higher relative sliding speed led to friction reduction, while a lower relative sliding speed resulted in increased wear. During sliding between the tool and the HSS sheet contact surface, the tool flattened a portion of the roughness peak on the work surface. This caused the work surface to be slotted, utilizing the worn debris as an intermediate, ultimately resulting in friction and wear due to interlocking and adhesion. Venema J [9, 10] reported that the cumulative wear effects occurred from one stretch test to the next, in addition to the fact that worn tool materials might be embedded in relatively soft sheet coatings and caused plow scratches on the tool contact surface. At higher temperatures, the dominant influence on the wear mechanism was attributed to the abrasive wear, while the adhesive wear exerted a significant impact on the wear mechanism at lower temperatures. In addition, the particles responsible for compaction wear mainly came from the fractured Al-Si coating and wear debris. Pelcastre L [11, 12] described the process of accumulation and compaction of wear fragments from Al-Si coatings as compaction galling. Mu Y. H [2] investigated the friction behavior of tool steel H13 and Al-Si-coated 22MnB5 boron steel under different conditions of temperature, sliding speed, contact pressure, and lubrication. The results revealed that the COF decreased significantly with the increase in temperature and contact pressure, but the sliding speeds had no significant effect on the COF. By studying the friction and wear mechanisms of the Al-Si coated HSS at high temperatures, the material transfers due to the adhesion of Al-Si coating and fragment compaction wear due to fracture were identified to be the main reasons for the tool surface wear. Therefore, improving the friction and wear properties of HSS sheets during the hot-stamping process can be realized by improving contact conditions and reducing material transfer between the Al-Si coating and the tool surface.

Laser surface texturing (LST) is a highly promising surface modification technique to improve the lubrication properties, friction contact states, and adhesion properties in friction contact interfaces of aluminum alloys, titanium alloys, and stainless steel. Podgornik B [13] studied the effects of surface roughness and LST on the friction and wear properties of tool steel, and found that

Table 1 The chemical composition (wt%) of the H13

Material	C	Si	Mn	Cr	Mo	W	S	P	Fe
H13	0.32~0.45	0.8~1.2	0.2~0.5	4.75~5.5	1.10~1.75	0.8~1.2	≤0.03	≤0.03	89.34~92.03

Table 2 The chemical composition (wt%) of the Usibor 1500P

Material	C	Si	Mn	Cr	Mo	W	S	P	Al	B	Fe
Usibor1500p	0.20~0.25	0.15~0.35	1.10~1.40	0.15~0.30	≤0.35	0.020~0.050	≤0.025	≤0.008	0.020~0.060	0.002~0.004	97.263~98.358

the micro-dimpled texture applied with appropriate density and contact lubrication provided excellent wear resistance. Kang et al. [14] studied the effects of micro-raised texture and micro-dimpled texture on the adhesion and wear properties of tool surface under dry friction conditions, and found that the high-density micro-raised texture had obvious anti-adhesion properties. Zheng K [15] proposed a method to improve the tensile properties of materials by using tools with surface texture in the process of hot stamping, and found that the texture parallel to the metal flow direction significantly improved the tensile properties. Cao Y [16] studied the influence of spraying deformation parameters on the friction and wear of HSS sheets under hot stamping conditions. It was observed that as the texture density increased, the average COF decreased first and then increased. Decrozant-Triquenaux J [17] investigated the synergic effect of high-temperature friction and wear on surface treatment either with or without lubrication. It was found that the tribological response strongly depended on the lubricant retention at the contact surface and the type of surface modification. Nevertheless, the application of LST in the hot stamping process of Al-Si-coated HSS is still understudied. Therefore, this study was conducted to investigate the influence and mechanism of LST on the friction reduction and wear resistance properties of the tool during hot stamping of Al-Si-coated HSS sheets. The findings of this study provide a theoretical basis and technical support for the application of LST in the hot stamping process of Al-Si-coated HSS, which can effectively improve the quality and efficiency of the process, thereby facilitating its application in the manufacturing industry.

2 Experimental set-up

2.1 Materials

In this study, H13 tool steel specimens were cut into cubes having a height of 10 mm and rounded corners having a diameter of 1 mm (Fig. 1). The specimens were polished and ultrasonic washed with anhydrous ethanol for 2 min, and the surface roughness was determined to be approximately 0.08 μm . The chemical composition (wt%) of the H13 used in this study (Baosteel Co., Ltd.) is shown in Table 1. After heat treatment, the hardness of the H13 specimens reached 53.2HRC. The 1.4 mm thick Usibor1500P Al-Si-coated HSS sheet (Baosteel Co., Ltd.) was cut to 20 mm width and 400 mm height. The chemical composition (wt%) of the HSS sheet in this study is given in Table 2.

2.2 Test specimens

Before the LST processing, the tool specimens were ultrasonic cleaned with anhydrous ethanol for 5 min, and then

Fig. 1 Schematic diagram of the LST dimension design

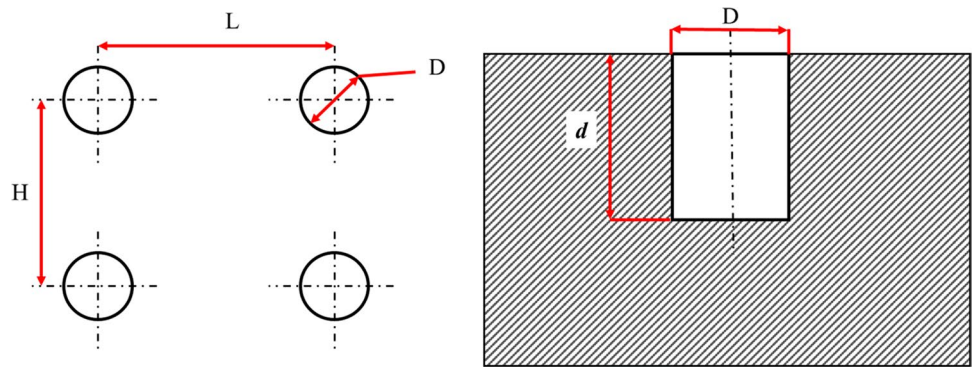


Table 3 LST dimension parameters

No.	L(mm)	H(μm)	D(μm)	d(μm)	Density (%)
1	140	140	50	50	10
2	99	99	50	50	20
3	81	81	50	50	30
4	70	70	50	50	40

dried for 2 h at 65°C. The LST specimens were prepared by nanosecond laser ablation. The schematic diagram of the laser texture dimension design is given in Fig. 1. According to the different LST densities of 10%, 20%, 30%, and 40%, four groups of LST specimens were fabricated, and the LST dimension parameters are shown in Table 3.

Fig. 2 3D model of the high-temperature strip-draw experiment

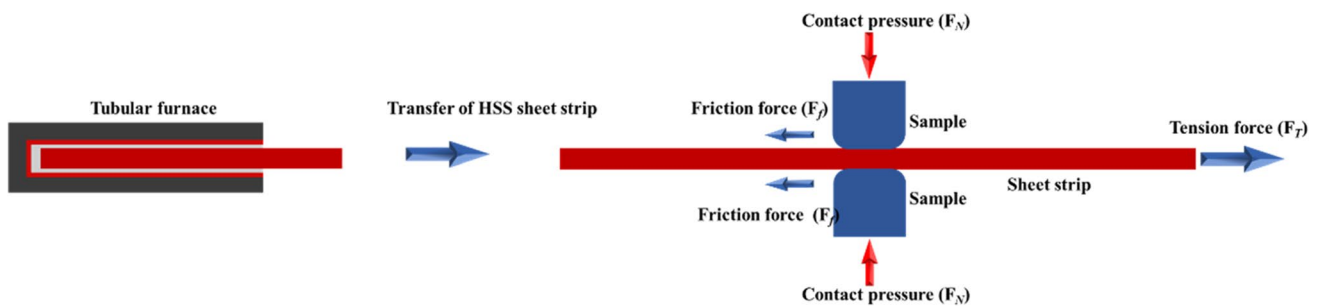
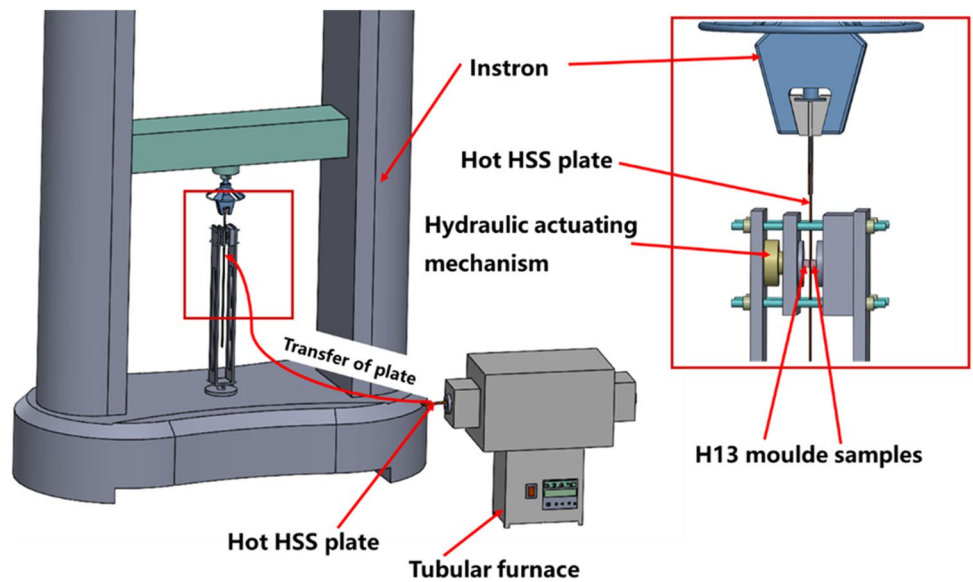


Fig. 3 Schematic diagram of the high-temperature strip-draw experiment

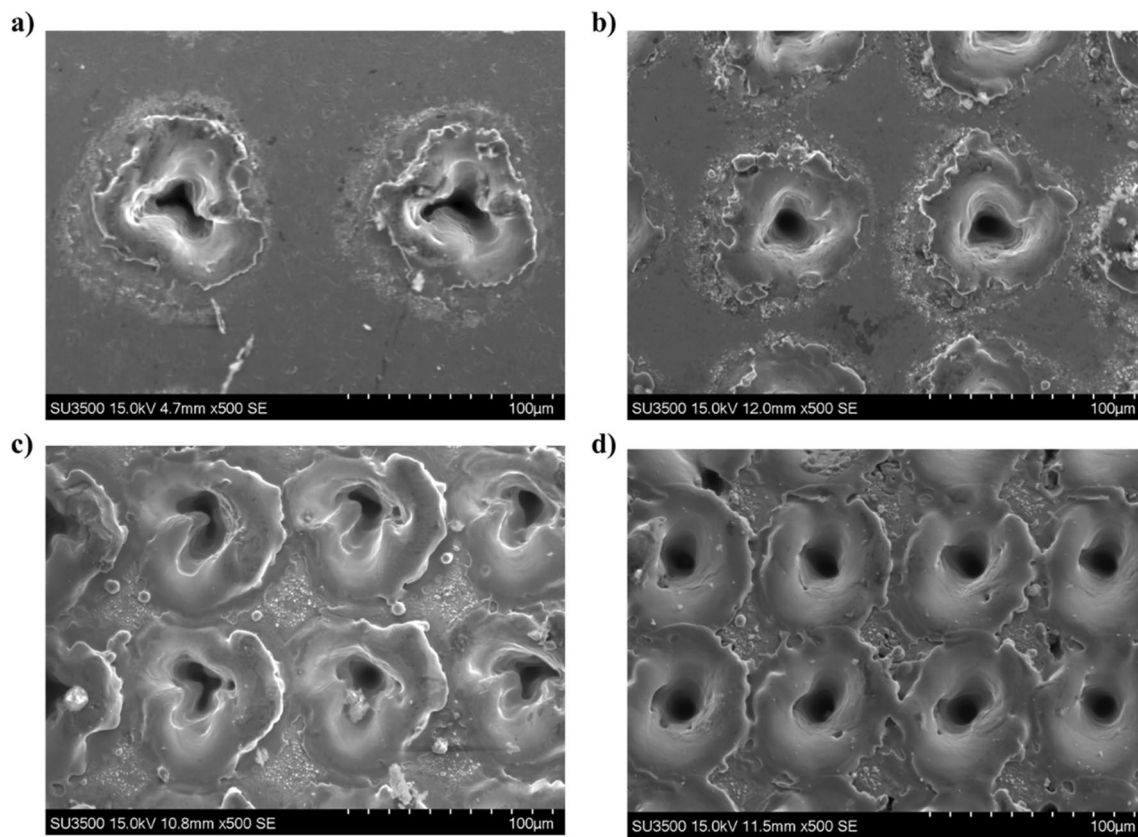


Fig. 4 2D morphologies of the LST specimens with different densities: **a** density 10%, **b** density 20%, **c** density 30%, **d** density 40%

2.3 Tribological test equipment

High-temperature strip-draw tribology experiments [5, 6] were carried out to investigate the friction and wear behavior of the interface between the tool with LST and Al-Si-coated HSS sheet under dry friction conditions at 700°C. To achieve the austenitizing temperature conditions of the Al-Si-coated HSS strip, the experimental process was designed to mimic the stamping process. The sheet material was first held in a tubular heating furnace at 940°C for 3 min. Within the specified time, the sheet material was then transferred to the friction testing machine (Fig. 2), and the friction experiment was conducted at 700°C under the temperature monitoring condition of the thermocouple (Fig. 3).

During the transfer process, the temperature of the high-strength steel plate decreases, and it rapidly cools down when it comes into contact with the mold having a lower temperature. When the upper mold comes into contact with the plate, plastic deformation and friction occur, and the temperature ranges from 600 to 730°C. After investigating sheet metal processing manufacturers (Shanghai Bohui Mould Co., LTD) and reviewing

relevant literature, the Auto Form simulation analysis determined that the representative temperature of friction occurrence was 700°C [18–22]. Therefore, the friction experiment was conducted after the sheet metal transfer and cooling to 700°C. The contact pressures of 5, 10, 15, and 20 MPa were applied respectively on both the LST and untextured specimens. The COF can be expressed by Eq. 1.

$$\mu = \frac{F_T}{2F_N} \quad (1)$$

2.4 Analysis technique

To analyze the friction and wear mechanism of LST, detailed observation and analysis of wear scratches are required. In this study, the 3D morphologies of the laser surface textures (LSTs) before and after the friction experiments were observed by the color 3D laser microscope VK9700K (Japan Keenshi Co., Ltd.). The wear scratches were analyzed by using the X-ray Energy Dispersive Spectrometer (EDS) and Tungsten filament scanning electron microscope (SEM) SU3500 (Tianmei (China) Scientific Instrument Co., Ltd.).

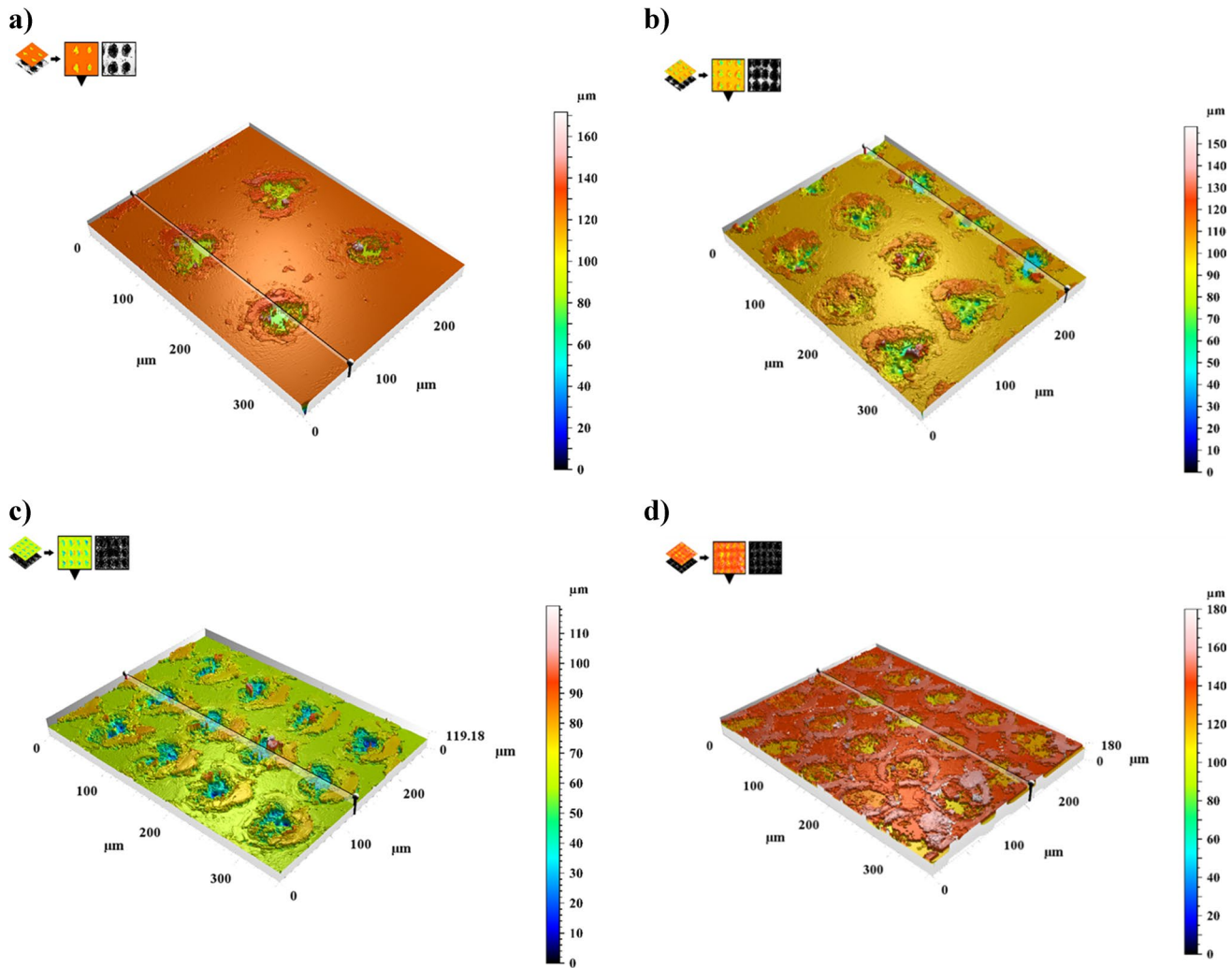


Fig. 5 3D morphologies of the LST specimens with different densities: **a** density 10%, **b** density 20%, **c** density 30%, **d** density 40%

3 Results and discussion

3.1 LST characterization

The 2D and 3D images of the LSTs and profile height curves are shown in Figs. 4, 5, and 6. After the LST process, burrs and metal oxide particles adhered to the metal's surface, where some of the laser-ablated steel materials accumulated at the edges of the circular dimple, and some of them oxidized and sputtered on the specimens. More materials accumulated on the edge of the circular dimples with the increasing density of LST.

3.2 LST characterization

3.2.1 COF analysis

High-temperature friction experiments were conducted at a temperature of 700°C, with a sliding speed of 10 mm/s

between the tool and the Al-Si-coated HSS sheet. The COF curves of the untextured and LST specimens are shown in Fig. 7. It can be seen that the COF of the original specimens increased with the increasing contact pressure. Meanwhile, the COF of the LST specimens was lower than that of the untextured specimens, indicating an excellent friction reduction effect of LST. The running-in periods for the untextured specimens exceeded 50 mm (5s) and they extended with the increase in contact pressures. In contrast, textured specimens exhibited running-in periods shorter than 10 mm (1s), and showed minimal change with the increase in contact pressure and LST density. The average COF values are presented in Fig. 7c. At the same LST density, the COF increased first and then decreased with the increasing contact pressure. At the same contact pressure, the average COF decreased first and then increased with the increasing surface texture density. For the LST specimens with 30% density subjected to the friction experiments, the average COF reached minimum

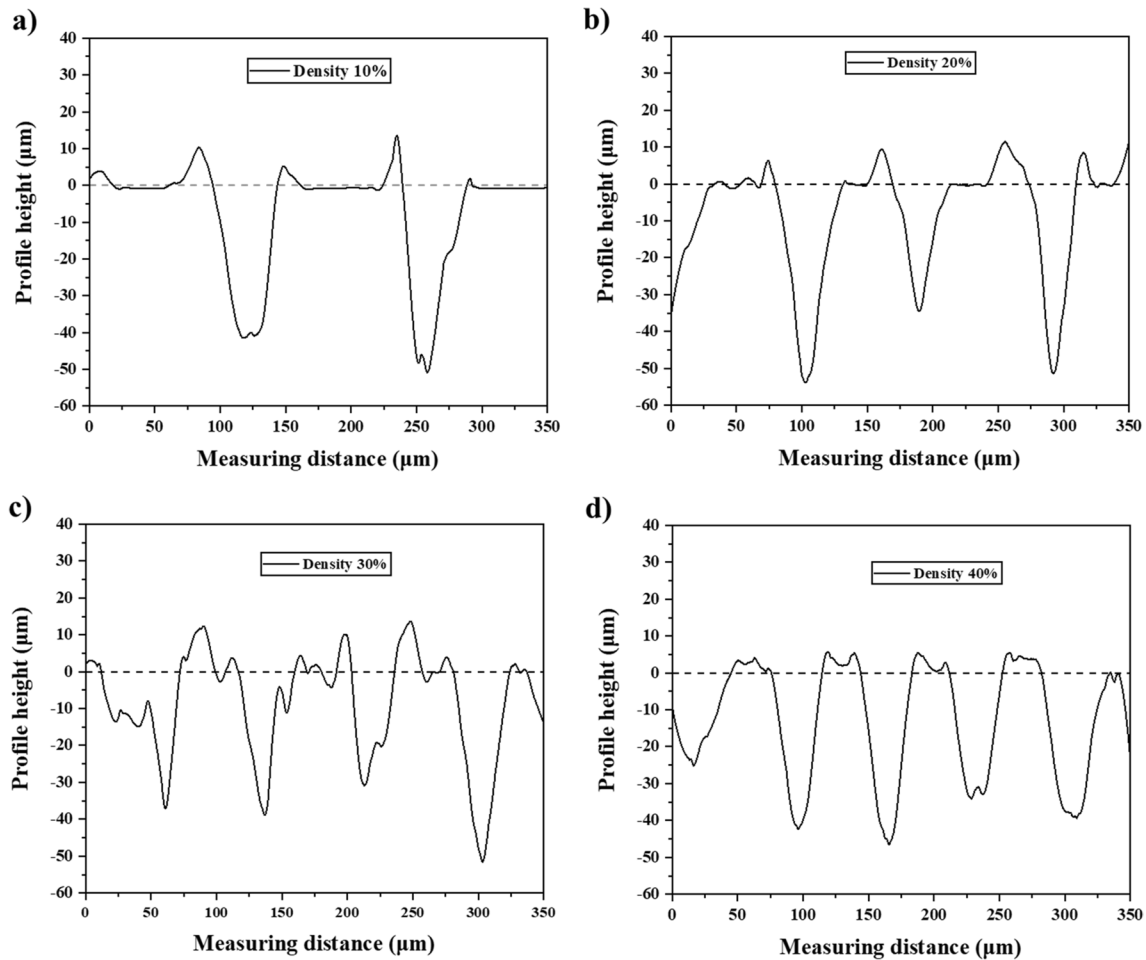


Fig. 6 Profile heights of the LST specimens with different densities: **a** 10% density, **b** 20% density, **c** 30% density, **d** 40% density

values of 0.197, 0.292, 0.319, and 0.242 at pressures of 5 MPa, 10 MPa, 15 MPa, and 20 MPa, respectively. These values were significantly lower than those of the untextured specimens by approximately 64.62%, 52.3%, 51.9%, and 67.11%, respectively. These results indicate that the LST process can significantly reduce the COF of the tool on the Al-Si-coated HSS strips at high temperatures. With a fixed contact pressure, the COF decreased and then increased with the increasing LST density. The smallest COF was consistently observed at a 30% LST density, irrespective of the varying contact pressures. Therefore, the LST process can effectively improve the anti-friction and wear resistance performance of the Al-Si-coated HSS sheets at high temperatures and high contact pressures.

3.2.2 Wear scratches analysis

A color 3D laser microscope VK9700K was used in this study to observe the 3D morphology and surface profile height curves of wear scratches for the untextured

specimens after the friction experiments. It was found that the layer-by-layer adhesion and flattened adhesion occurred on the surface of the untextured specimens after the friction experiments at the contact pressure of 5 MPa (Fig. 8a). The adhesion materials accumulated during sliding after the friction experiments at the contact pressure of 10 MPa (Fig. 8b). Subsequently, the bulk adhesion materials accumulated, flattened, and formed more even tiled adhesion at the contact pressure of 15 MPa (Fig. 8c). Spalling scratches and plowing grooves on the flattened adhesion occurred on the wear scratches at the contact pressure of 20 MPa (Figs. 8d and 9).

After conducting the friction experiments on LST specimens with different densities at various contact pressures, a laser confocal roughness measurement system Leica DCM8 was used to obtain the 3D morphologies and surface profile height curves of the wear scratches.

After the friction experiments at 5 MPa, prominent adhesion materials were observed filling in the dimples on the wear scratches of LST specimens with 10% density

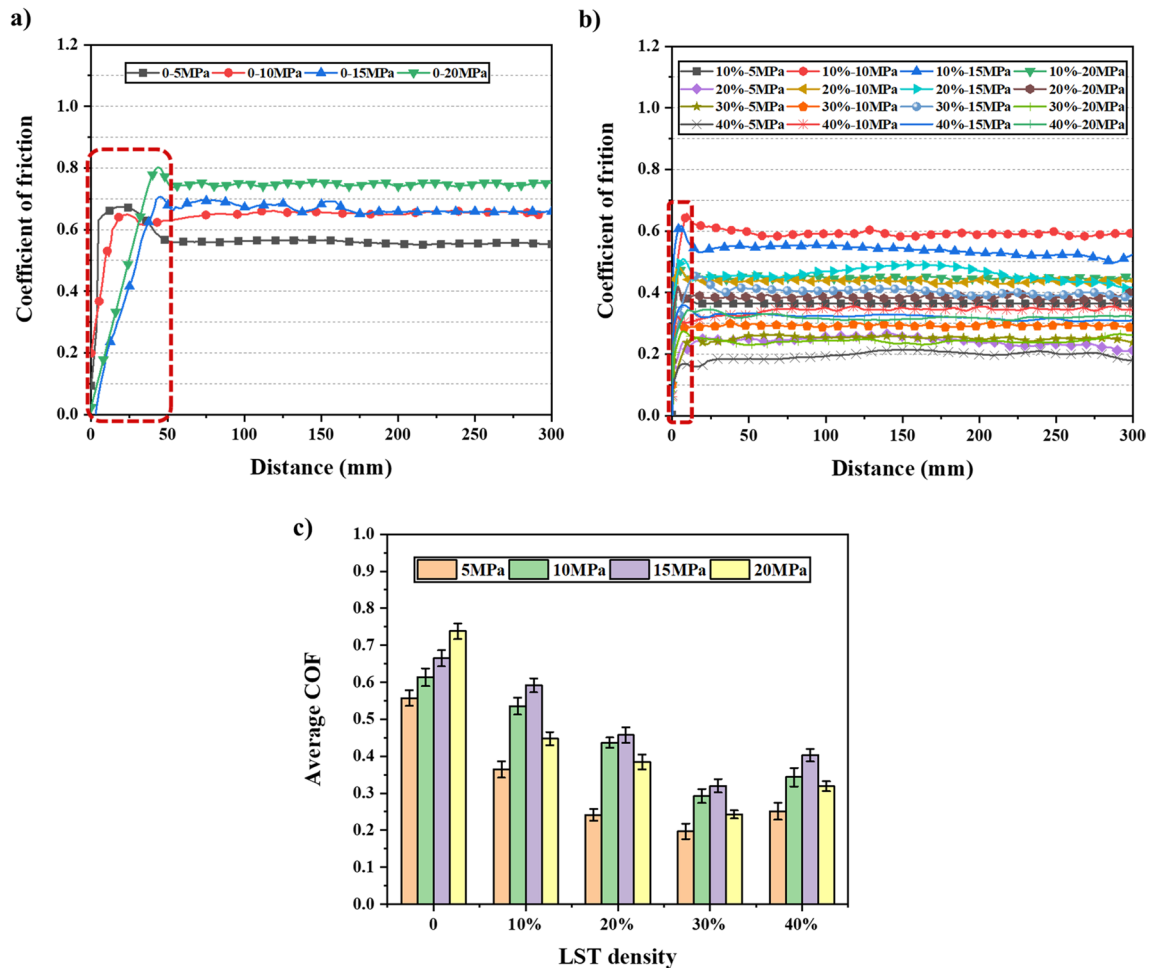


Fig. 7 COF curves of the untextured and LST specimens: **a** COF curves of the untextured specimens, **b** COF curves of the LST specimens, **c** Average COF bar diagrams

(Figs. 10a and 11). After the friction experiments at 10 MPa, layer-by-layer deposition of adhesion materials was clearly observed around the dimples along the sliding direction on the wear scratches of LST specimens with 10% density (Figs. 10b and 11). As the contact pressure increased from 5 to 15 MPa, the adhesion materials were flattened, resulting in smoother wear scratches. However, at the pressure of 20 MPa, the wear scratches exhibited obvious scratches and spalling of adhesion materials (Fig. 10c and d). The wear scratches on LST specimens with 10% density after the friction experiments at 10 MPa and 15 MPa were smoother compared to those at the pressures of 5 MPa and 20 MPa. This is because the adhesion materials first accumulated around the dimples at 5 MPa, and then flattened and spread to the unconnected areas between the dimples with the increasing contact pressure. Subsequently, the adhesion materials were crushed to form

fragments adhering to the tool surface. In addition, peeling wear occurred due to the fracturing of adhesion material and the plow wear of the hard phase pressed into the contact surface of the coating at 20 MPa [20] (Fig. 10c and d). The adhesion material was mainly concentrated near the dimples, some of which were filled by the debris. However, in the case of LST specimens with 10% density at 5 MPa and 10 MPa, the areas between the dimples did not contact with the wear scratches. The increase in contact area and material adhesion resulted in an increase in the friction coefficient. At a contact pressure of 20 MPa, both the contact area and material adhesion reached their maximums, leading to adhesive material fracture due to friction. This subsequently led to dominant wear friction characterized by furrows, resulting in a slight reduction in the friction coefficient. The depth (d) of all the dimples was lower than 20 μm after the friction experiments

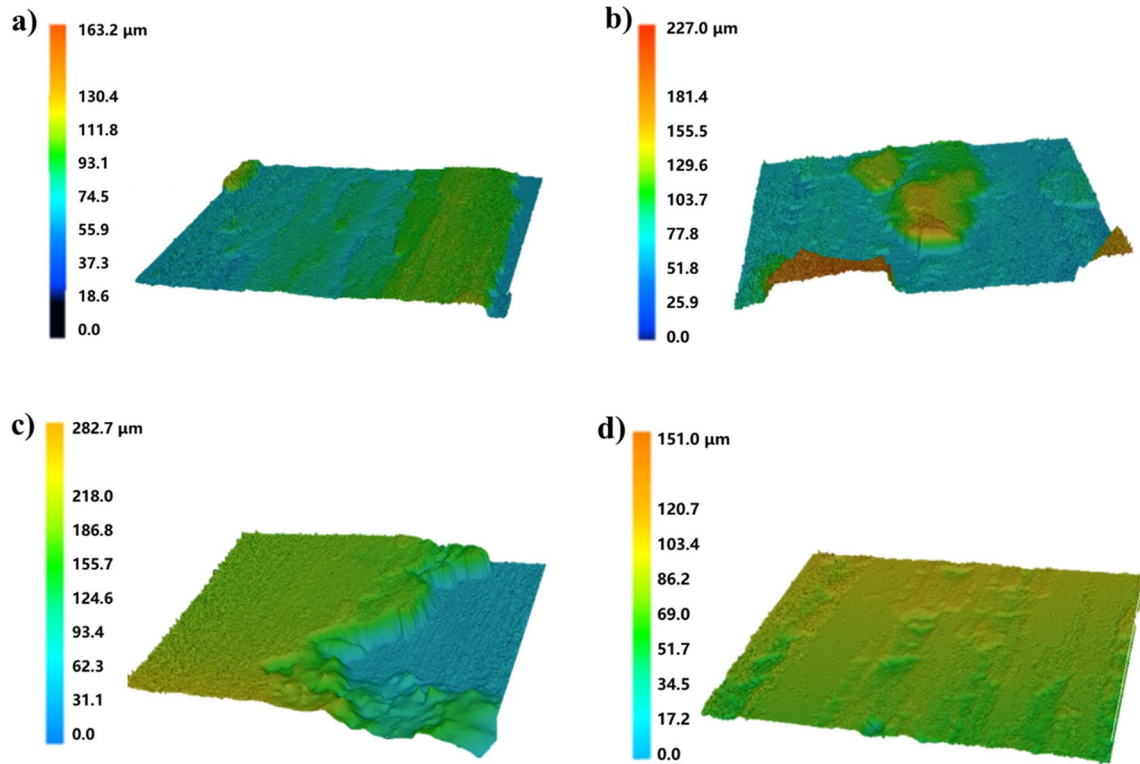


Fig. 8 3D morphologies of the untextured specimens after the friction experiments at different contact pressures of **a** 5 MPa, **b** 10 MPa, **c** 15 MPa, and **d** 20 MPa

(Fig. 11). This proves that LST has a significant effect on the accumulation of fractured Al-Si coating and wear debris during the friction process, as well as on the reduction of adhesion of the Al-Si coating on the friction contact surface and wear scratches of the tool.

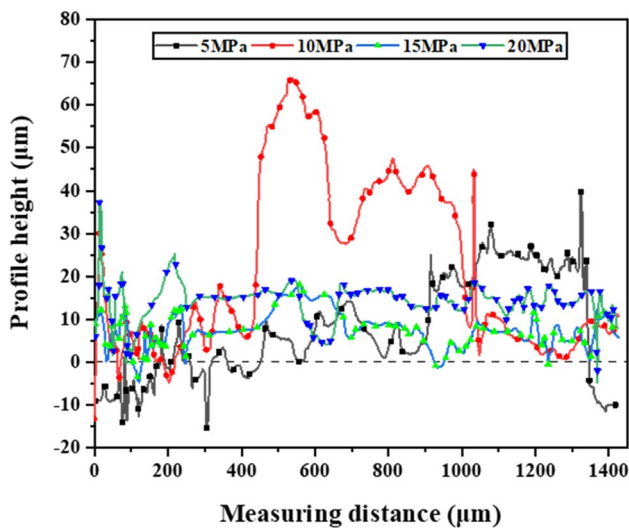


Fig. 9 Surface profile height curves of the untextured specimens after the friction experiments at different contact pressures

The wear scratches on the LST specimens with 20% density were smoother than those on the LST specimens with 10% density at 5 MPa and 10 MPa, while having no uncontacted areas between dimples, and the dimples were filled (Fig. 12a and b). These observations prove that high-density dimples can prevent the concentrated accumulation of adhesive materials, which also explains the significant reduction in the COF of the LST specimens with 20% density. Analyzing the increasing average COF phenomenon (Fig. 7c), the COF of adhesion friction between adhesion materials and Al-Si coating was found to be greater than that of the furrow friction, which was the reason for the increase in COF at the pressure of 20 MPa (Fig. 13).

The wear scratches on LST specimens with 30% density exhibited more furrows and scratches, with less material accumulation compared to the LST specimens with 20% density. Furthermore, observing the average coefficient of friction (COF), it became evident that the furrow friction surpassed adhesion friction as the prevailing mechanism, resulting in a decrease in the coefficient of friction. Less adhesion material was observed on the wear scratches of the LST specimens with 30% density compared to the LST specimens with 20% density (Fig. 14). Meanwhile, a decrease in adhesive wear and an increase

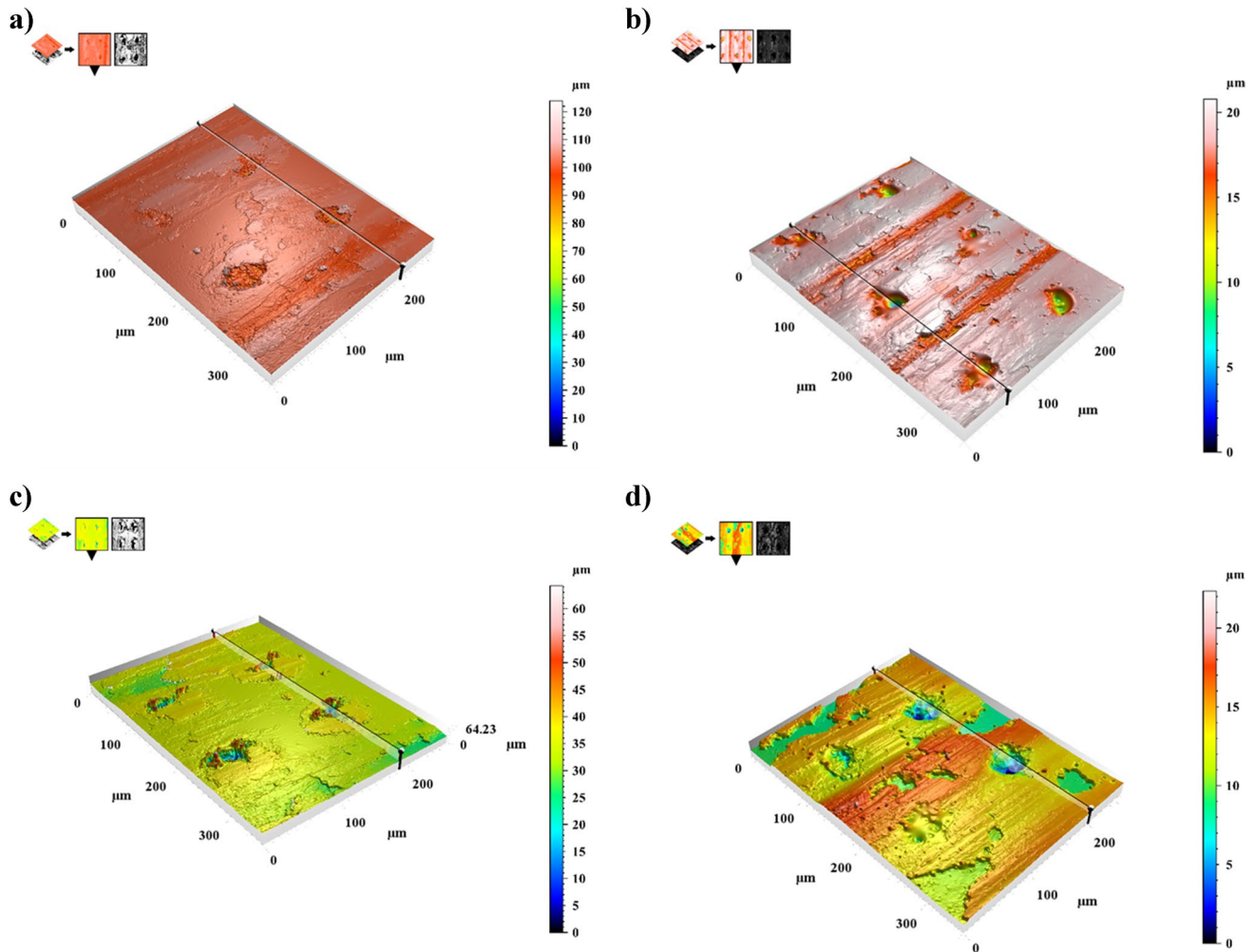


Fig. 10 3D morphologies of the LST specimens with 10% density after the friction experiments at different contact pressures of **a** 5 MPa, **b** 10 MPa, **c** 15 MPa, and **d** 20 MPa

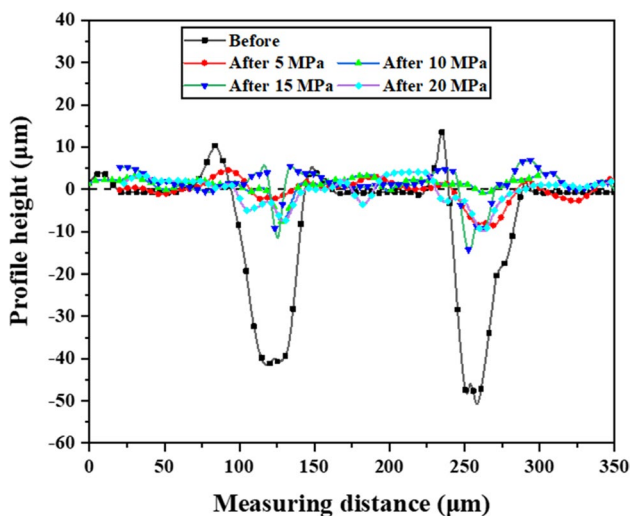


Fig. 11 Surface roughness curves of the LST specimens with 10% density after the friction experiments at different contact pressures

in furrow wear were observed on the wear scratches of LST specimens with 30% density compared to those with 20% density. This reduction in adhesive wear was also consistent with the decrease in the average COF. These findings highlight the fact that the high-temperature friction force between the Al-Si-coated HSS sheet and the H13 tool is mainly because of the coating's adhesion friction force [7] (Fig. 15).

The dimple filling level of the LST specimens with 40% density was observed to be higher compared to those of 30% density. This is because the actual contact area decreased due to the higher dimple density, and the actual contact pressure between the friction contact surfaces increased, resulting in the increase of the COF (Fig. 7c). Thus, more scratches appeared on the surface adhesion material of the LST specimens with 40% density (Figs. 16 and 17) which is consistent with the results of the average COF (Fig. 7c).

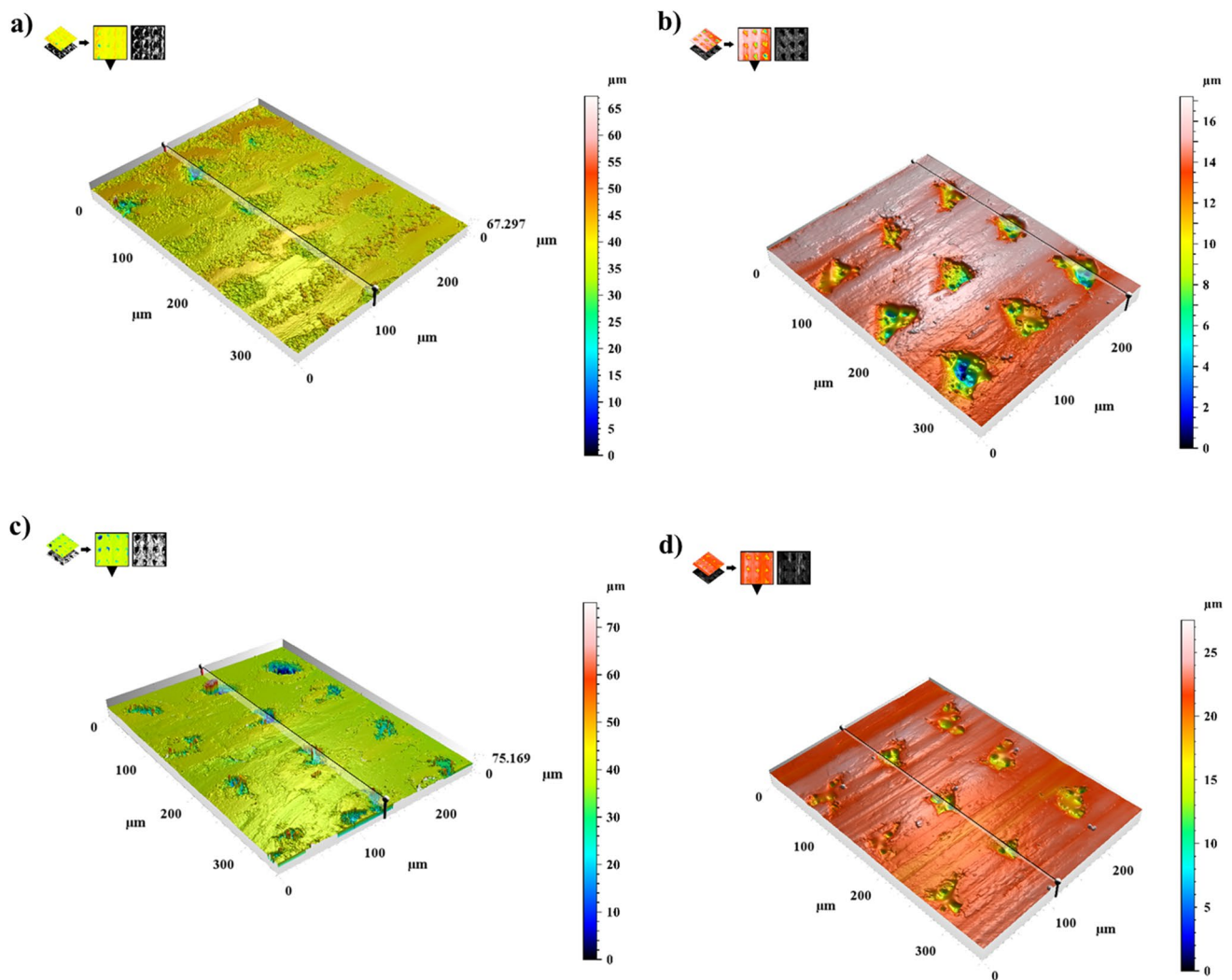


Fig. 12 3D morphologies of the LST specimens with 20% density after the friction experiments at different contact pressures of **a** 5 MPa, **b** 10 MPa, **c** 15 MPa, and **d** 20 MPa

3.3 Friction and wear mechanism

To further understand the surface adhesion and scratches on the wear scratches of the specimens with or without LST after friction, as well as explain the friction reduction and wear resistance mechanism, tungsten filament scanning electron microscopy (SEM) with X-ray Energy Dispersive Spectrometer (EDS) was used to analyze the wear scratches of the original specimens at different contact pressures (Fig. 18) and different densities (Figs. 19, 20, 21, and 22).

Figure 18 shows the SEM images and the EDS results of the untextured specimens after the friction experiments at the pressures of 5, 10, 15, and 20 MPa. When the contact pressure was 5 MPa (Fig. 18a), the surface

adhesion material accumulated layer-by-layer on the tool contact surface with the increase in friction, and the wear debris mainly appeared on the thick adhesion material area, identified as A1. When the contact pressure was 10 MPa (Fig. 18b), slight furrow wear occurred on the wear scratches of the untextured specimens. The primary mechanism of friction was adhesive wear, wherein the contact pressure induced flattening, peeling, and fracturing of the adhesive material. Consequently, the furrow wear and peeling wear occurred on the interface between the mold and its contact surface. As the pressure reached 20 MPa (Fig. 18d), the furrow wear became predominant while the adhesive wear acted as a supporting factor. The debris resulting from adhesive damage significantly contributed to the severe furrow wear observed on the wear

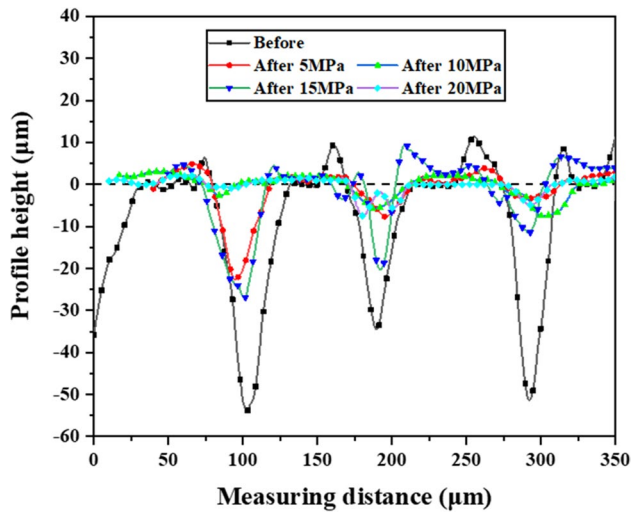


Fig. 13 Surface roughness curves of the LST specimens with 20% density after the friction experiments at different contact pressures

scratches. It may be caused by the breaking of the Al-Si coating and large adhesion material during friction [20]. During this period, a part of the debris was ground and filled into the furrow again, which reduced the wear condition of the surface and the non-uniformity of the surface. This indicated that the adhesion effect of the coating on the tool surface and wear debris causing furrow wear was mainly due to the Al element in the Al-Si coating.

Figure 19 presents the SEM and EDS results for wear scratches of the LST specimens with 10% density after the friction experiments at pressures of 5, 10, 15, and 20 MPa. The adhesion material on the wear scratches of LST specimens with 10% density at 5 and 10 MPa first accumulated around the dimple. Less adhesion occurred in the void part of the dimples, creating non-contact depressions, while the rupture of adhesive materials and accumulation of friction debris resulted in the formation of new adhesions (Fig. 19a and b). When the contact

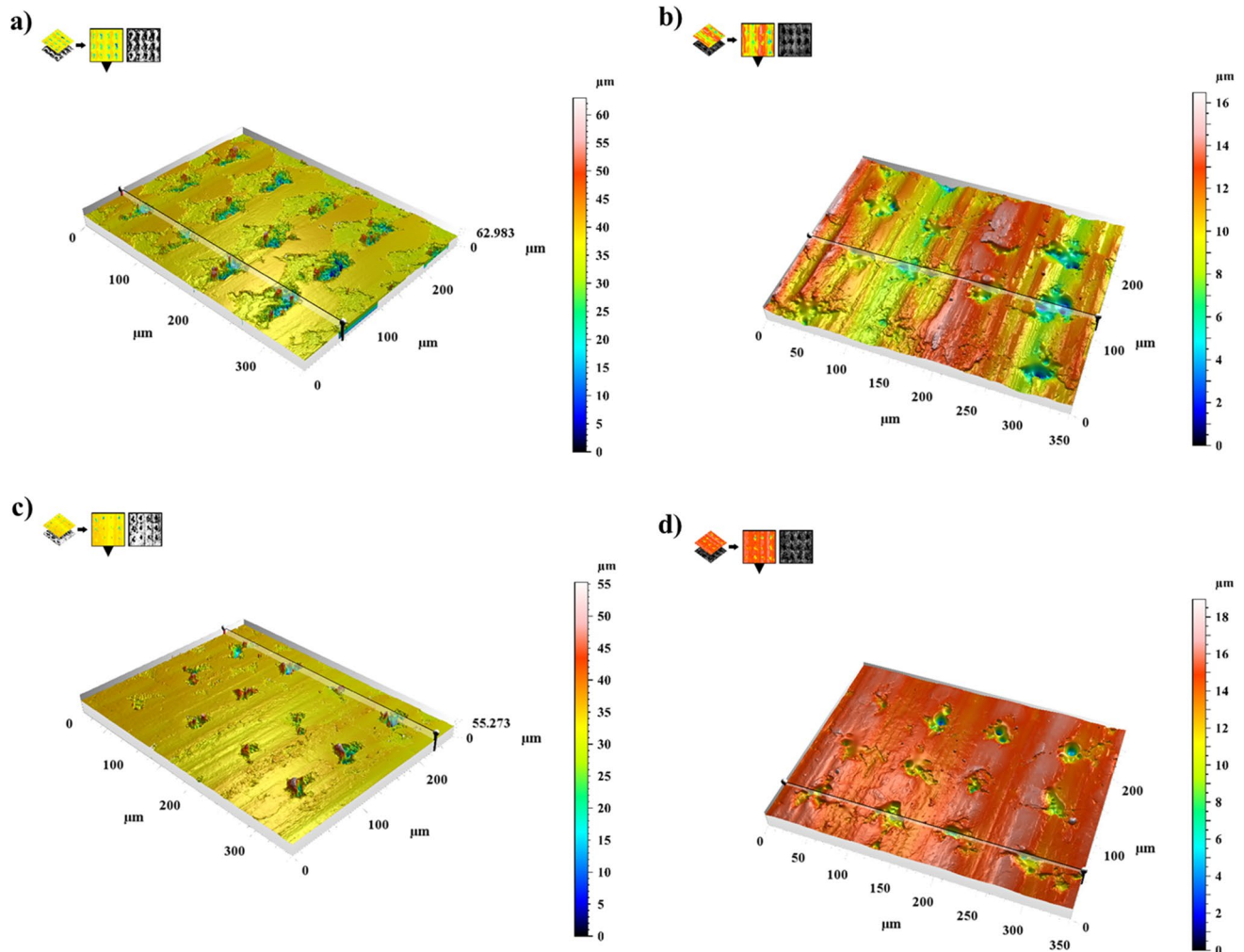


Fig. 14 3D morphologies of the LST specimens with 30% density after the friction experiments at different contact pressures of **a** 5 MPa, **b** 10 MPa, **c** 15 MPa, and **d** 20 MPa

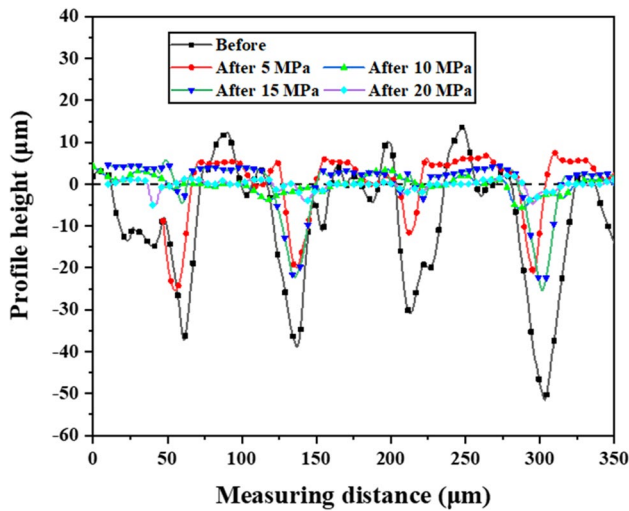


Fig. 15 Surface roughness curves of the LST specimens with 30% density after the friction experiments at different contact pressures

pressure was higher than 15 MPa (Fig. 19c), the adhesion material around the dimple flattened, and the accumulation of adhering material around the dimple extended to the surface of the dimples. This reduced the opening area of the dimple and promoted the difficulty of accumulating the frictional debris from the dimples. More wear debris, plowing wear, and grooves appeared on the wear scratches of the LST specimens with 10% density after the friction experiments at pressures of 15 and 20 MPa (Fig. 19d).

The adhesion material on the wear scratches of LST specimens with 20% density, observed after the friction experiments (Fig. 20), initially accumulated layer-by-layer around the dimples, similar to the wear scratches of LST specimens with 10% density after the friction experiments at 5 MPa (Fig. 20a). The debris and fractured adhesion material accumulated near the dimples and were collected by the dimples. When the contact pressure was

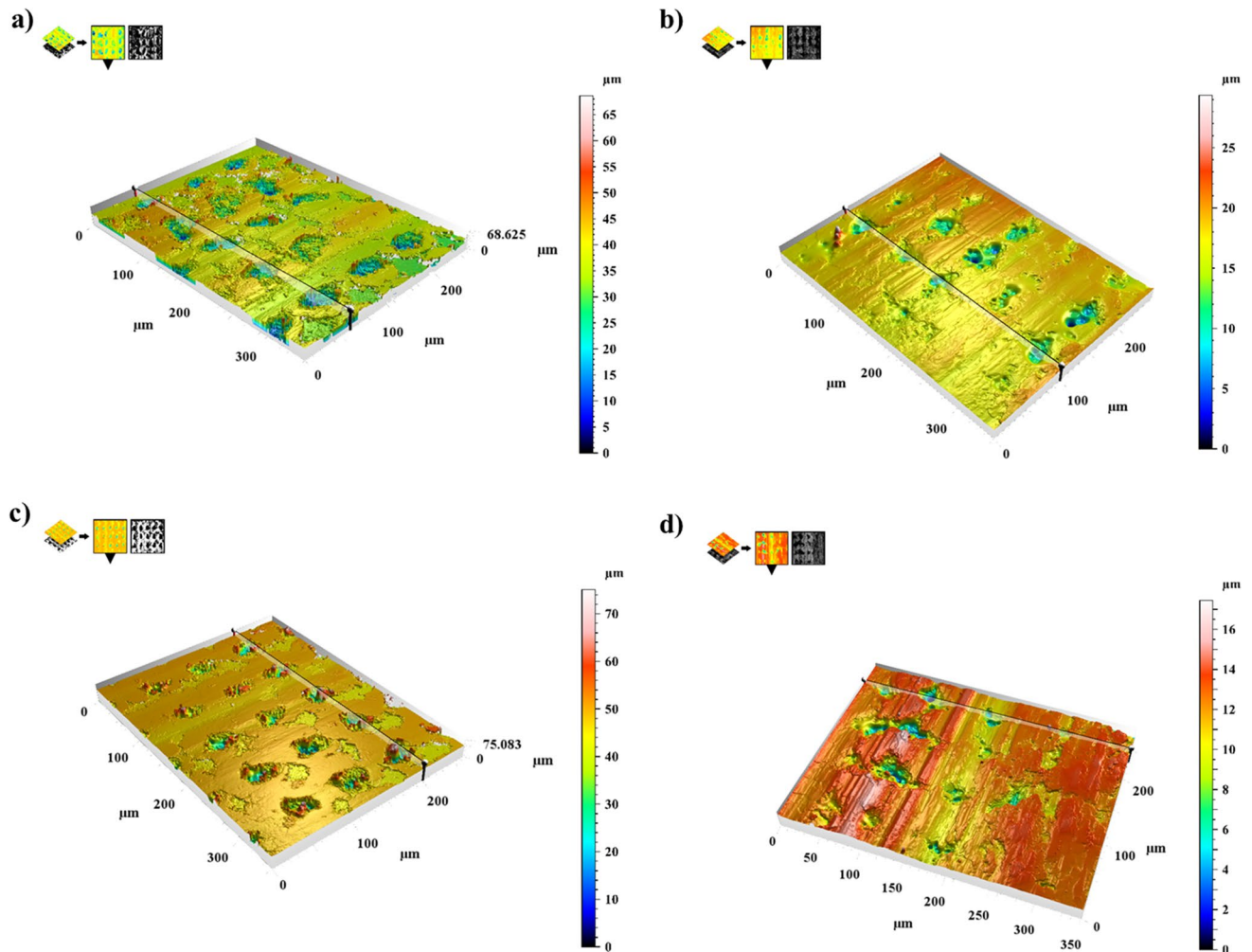


Fig. 16 3D morphologies of the LST specimens with 40% density after the friction experiments at different contact pressures of **a** 5 MPa, **b** 10 MPa, **c** 15 MPa, and **d** 20 MPa

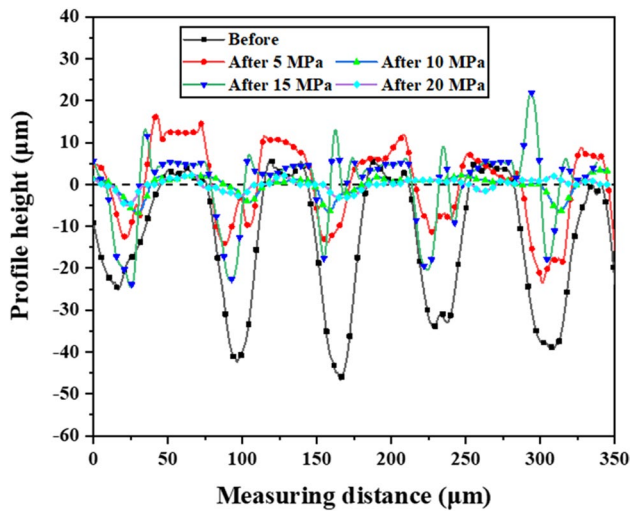


Fig. 17 Surface roughness curves of the LST specimens with 40% density after the friction experiments at different contact pressures

increased to 15 MPa (Fig. 20c), furrow grooves and fractured adhesion material appeared on the wear scratches. When the contact pressure was 20 MPa (Fig. 20d), the debris was flattened under the increased contact pressure and adhered to the friction contact surface, which could be collected by the dimples alternatively.

The higher density of 30% in the LST specimens reduced the adhesion material on the wear scratches after the friction experiments (Fig. 21) and enhanced the ability of the dimples to contain debris. At the contact pressure of 10 MPa, slight furrow grooves occurred on the wear scratches (Fig. 21b). At the contact pressure of 20 MPa (Fig. 21d), an increased presence of Fe elements in the dimple-filling material indicated an elevated amount of tool surface wear with the increasing contact pressure. Thus, more wear debris was created and the dimple opening was reduced with the increase in contact pressure.

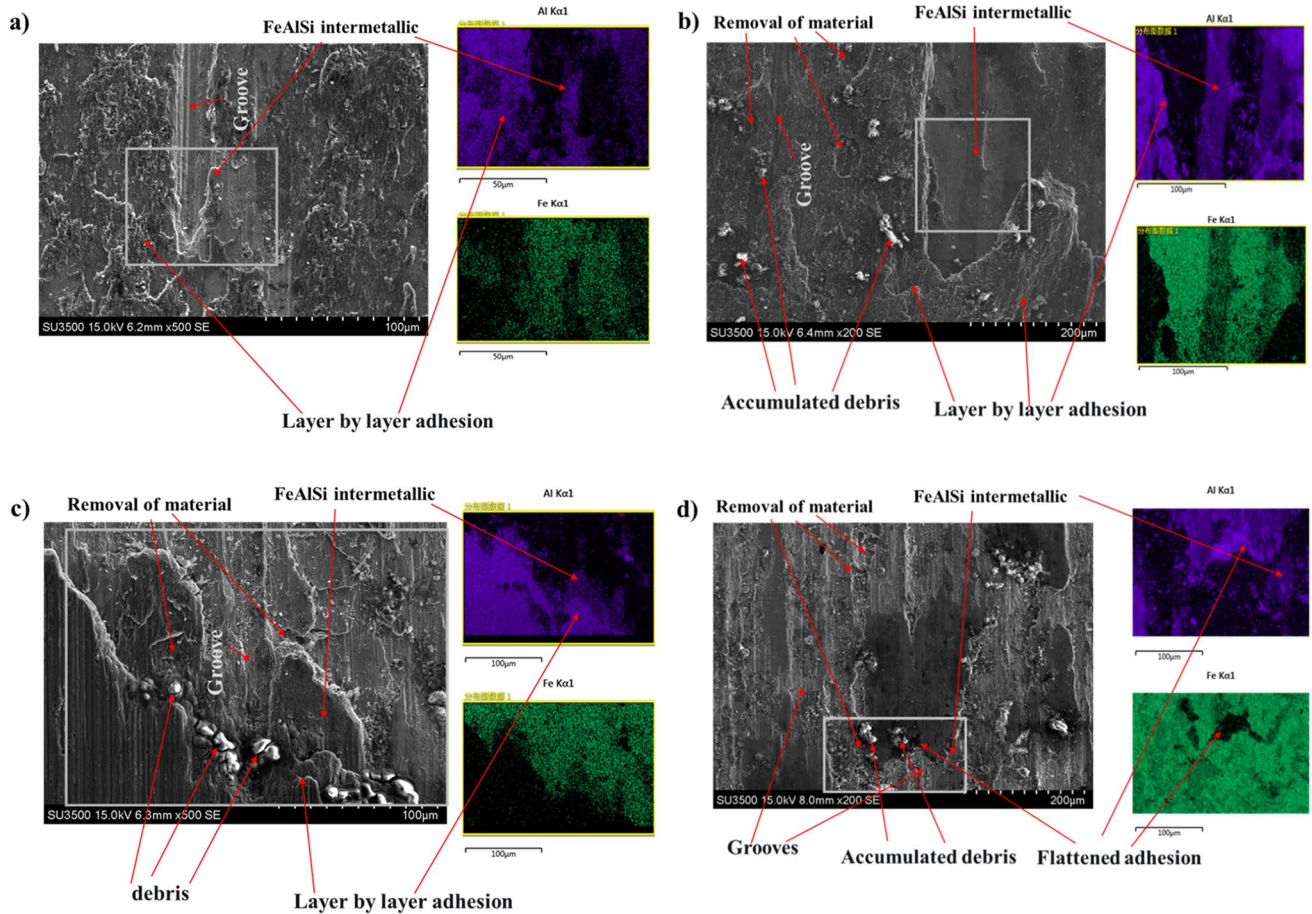


Fig. 18 SEM images and EDS elemental analysis of the frictional surfaces for the untextured specimens at the contact pressures of **a** 5 MPa, **b** 10 MPa, **c** 15 MPa, and **d** 20 MPa

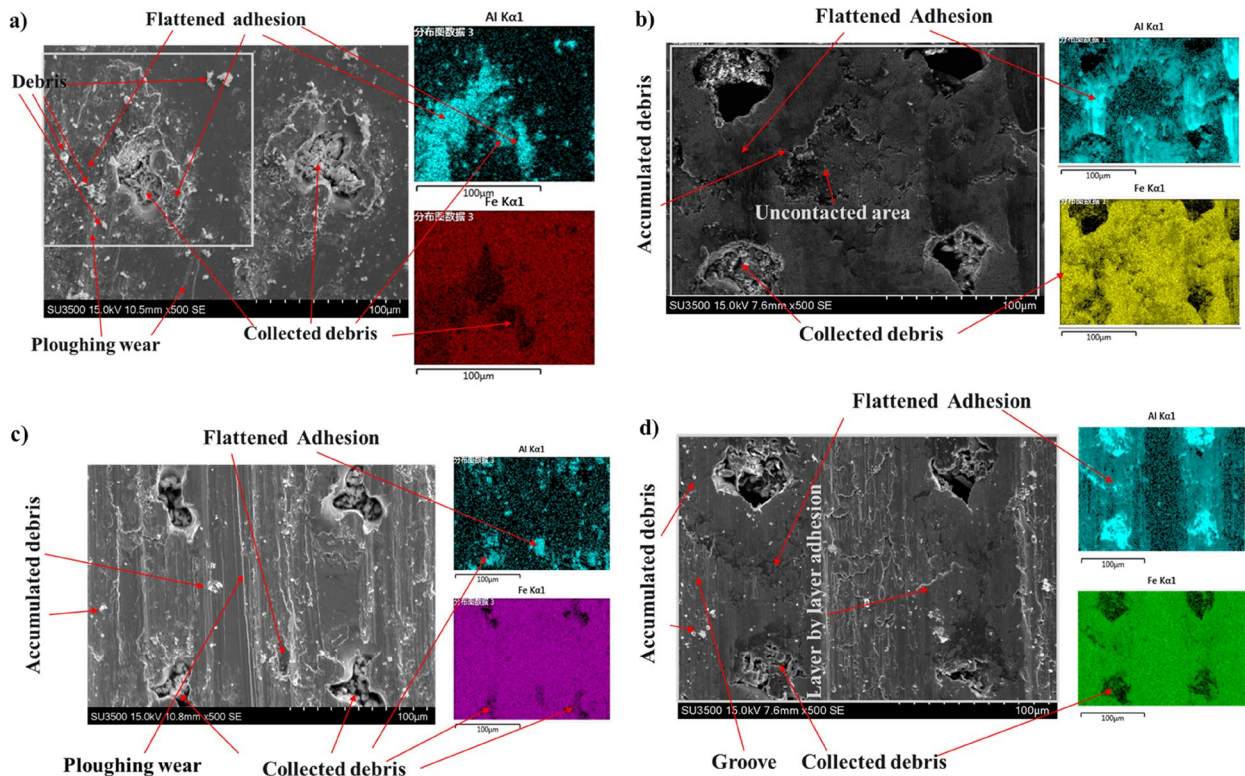


Fig. 19 SEM images and EDS elemental analysis of wear scratches after friction for the LST specimens with 10% density at the contact pressures of **a** 5 MPa, **b** 10 MPa, **c** 15 MPa, and **d** 20 MPa

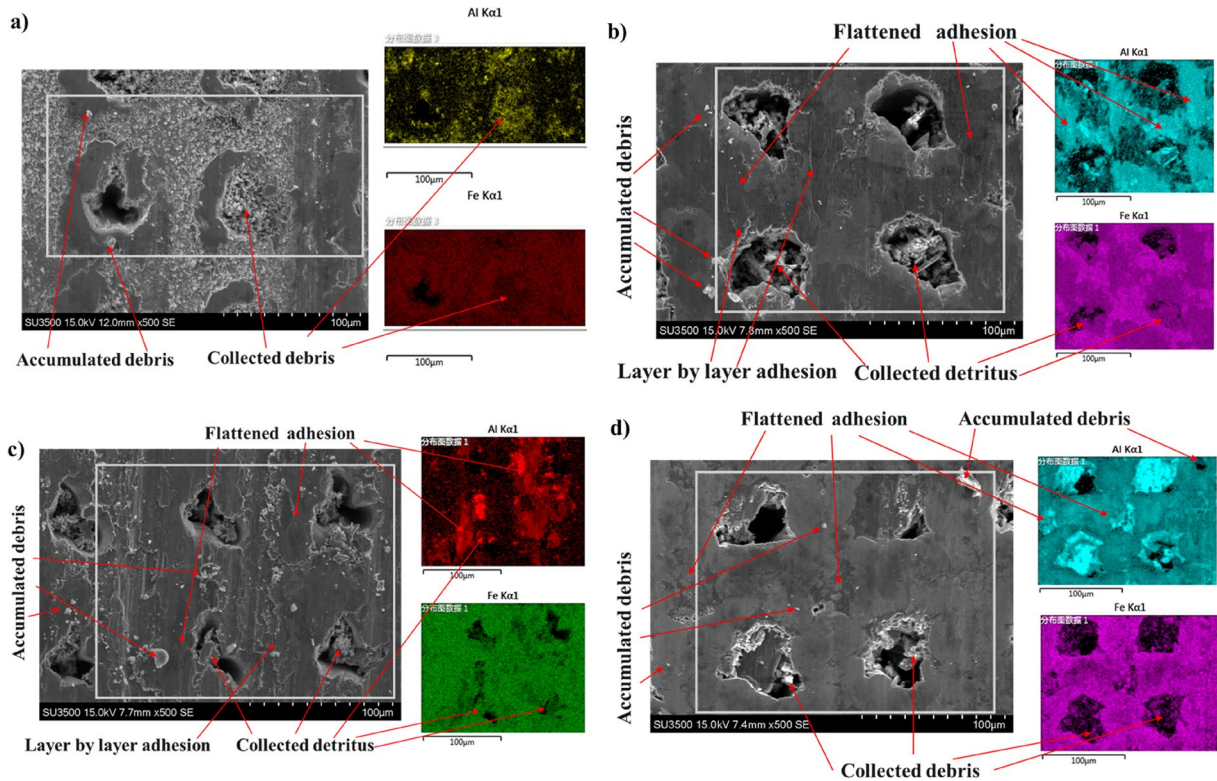


Fig. 20 SEM images and EDS elemental analysis of wear scratches after friction for the LST specimens with 20% density at the contact pressures of **a** 5 MPa, **b** 10 MPa, **c** 15 MPa, and **d** 20 MPa

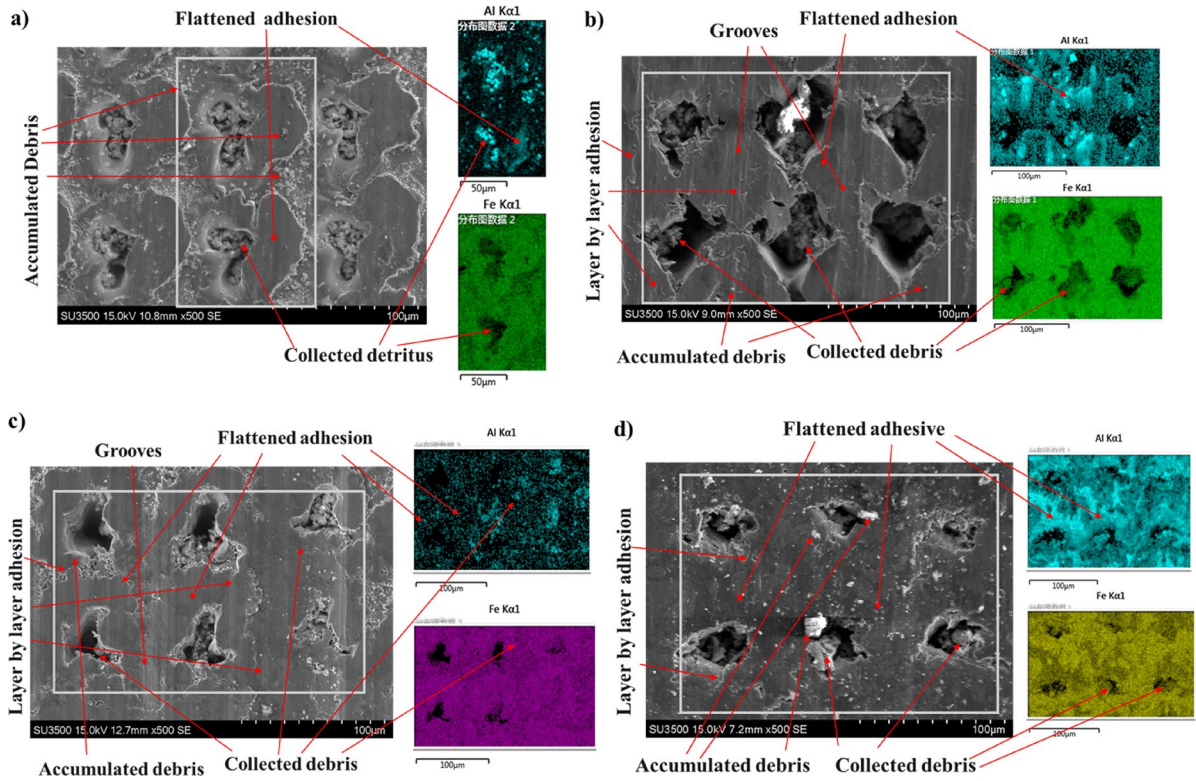


Fig. 21 SEM images and EDS elemental analysis of wear scratches after friction for the LST specimens with 30% density at the contact pressures of **a** 5 MPa, **b** 10 MPa, **c** 15 MPa, and **d** 20 MPa

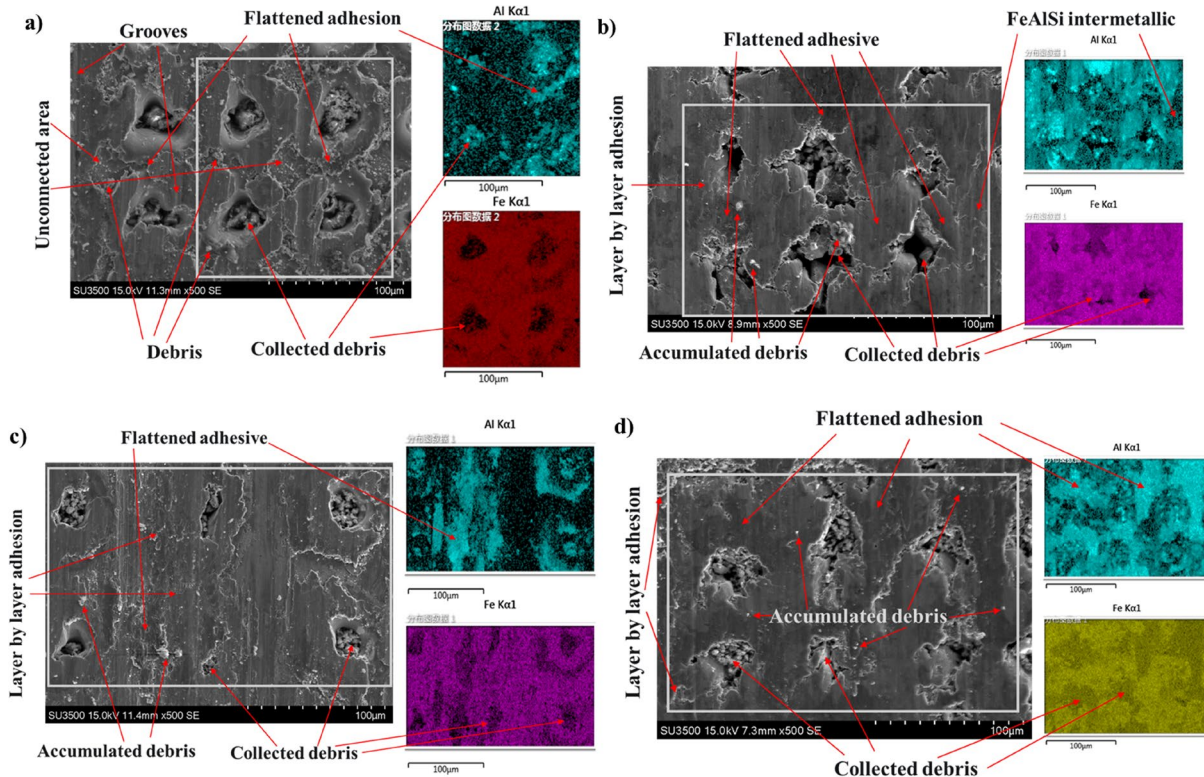


Fig. 22 SEM images and EDS elemental analysis of wear scratches after friction for the LST specimens with 40% density at the contact pressures of **a** 5 MPa, **b** 10 MPa, **c** 15 MPa, and **d** 20 MPa

More debris accumulated in the dimples on wear scratches of LST specimens with 40% density after the friction experiments (Fig. 22). The dimple opening decreased, and a higher amount of debris was observed in the case of LST specimens with 40% density compared to the low-density LST specimens, indicating a reduction in the wear resistance effect of LST with 40% density. This can be attributed to the fact that the real contact pressure increased with the increase in the LST specimen density.

4 Conclusions

This study presents an investigation on the friction and wear behavior of H13 tool steel and Al-Si-coated HSS sheets with or without Laser Surface Texturing (LST) at high temperatures utilizing strip-draw friction experimental equipment. The study primarily focused on analyzing the influence and mechanisms of different densities of LST on the friction reduction and wear resistance of Al-Si-coated HSS sheets during high-temperature friction by analyzing the COF curves and wear scratches.

The key findings of this study are as follows:

- (1) The LST significantly reduces friction between the Al-Si-coated HSS sheet and the H13 tool contact interface under high temperature and high contact pressure conditions. Additionally, the running-in period of the LST specimens is shorter than that of the untextured specimens. Moreover, the average COF demonstrates significant reductions than those in the untextured specimens, particularly at an LST density of 30%
- (2) The wear mechanism between the Al-Si coating and the tool at high temperatures is primarily dominated by adhesive wear, with minor three-body wear. The adhesion of the material to the friction contact surface of the tool occurs layer by layer during the friction process, while the source of the three-body wear is a hard phase combined with the adhesion material and fragmentation from the tool.
- (3) The LST effectively reduces friction and wear by minimizing the adhesion of the Al-Si coating to the tool surface and the wear debris entering into the friction contact interface under high-temperature conditions

Author contribution All authors contributed to the study's conception and design. Material preparation, data collection, and analysis were performed by Tangjie Mei. The first draft of the manuscript was written by Tangjie Mei and all authors commented on the previous versions of the manuscript. All authors read and approved the final manuscript.

Funding This work was supported by the National Natural Science Foundation of China (Project No. 51875441), the Fundamental Research Funds for the Central Universities (No. zrzdz2017027).

Data availability The authors confirm that the data supporting the findings of this study are available within the article.

Declarations

Competing Interests The authors declare no competing interests.

References

1. Zhang W, Xu J (2022) Advanced lightweight materials for Automobiles: A review. *Mater Des* 221:110994. <https://doi.org/10.1016/j.matdes.2022.110994>
2. Mu Y, Simonetto E, Scagnolari M, Ghiotti A (2020) Wear in Hot Stamping by Partition Heating. *JMMP* 4:18. <https://doi.org/10.3390/jmmp4010018>
3. Guo M, Gao K, Wang W, Wei X (2017) Microstructural evolution of Al-Si coating and its influence on high temperature tribological behavior of ultra high strength steel against H13 steel. *J Iron Steel Res Int* 24:1048–1058. [https://doi.org/10.1016/S1006-706X\(17\)30152-8](https://doi.org/10.1016/S1006-706X(17)30152-8)
4. Boher C, Le Roux S, Penazzi L, Dessain C (2012) Experimental investigation of the tribological behavior and wear mechanisms of tool steel grades in hot stamping of a high-strength boron steel. *Wear* 294–295:286–295. <https://doi.org/10.1016/j.wear.2012.07.001>
5. Ghiotti A, Bruschi S, Medea F (2015) Comparison of tribological and wear performances of AlSi and Zn coatings in hot stamping of boron steel sheets. *Wear* 332–333:810–821. <https://doi.org/10.1016/j.wear.2015.01.046>
6. Ghiotti A, Sgarabotto F, Bruschi S (2013) A novel approach to wear testing in hot stamping of high strength boron steel sheets. *Wear* 302:1319–1326. <https://doi.org/10.1016/j.wear.2012.12.051>
7. Azushima A, Uda K, Yanagida A (2012) Friction behavior of aluminum-coated 22MnB5 in hot stamping under dry and lubricated conditions. *J Mater Process Technol* 212:1014–1021. <https://doi.org/10.1016/j.jmatprotec.2011.12.009>
8. Schwingenschlögl P, Merklein M (2020) Characterization of tribological conditions within direct hot stamping. *J Mater Process Technol* 278:116535. <https://doi.org/10.1016/j.jmatprotec.2019.116535>
9. Venema J, Hazrati J, Matthews DTA, et al (2018) The effects of temperature on friction and wear mechanisms during direct press hardening of Al-Si coated ultra-high strength steel. *Wear* 406–407:149–155. <https://doi.org/10.1016/j.wear.2018.04.006>
10. Venema J, Matthews DTA, Hazrati J, et al (2017) Friction and wear mechanisms during hot stamping of AlSi coated press hardening steel. *Wear* 380–381:137–145. <https://doi.org/10.1016/j.wear.2017.03.014>
11. Pelcastre L, Hardell J, Prakash B (2013) Galling mechanisms during interaction of tool steel and Al-Si coated ultra-high strength steel at elevated temperature. *Tribol Int* 67:263–271. <https://doi.org/10.1016/j.triboint.2013.08.007>
12. Pelcastre L, Hardell J, Prakash B (2011) Investigations into the occurrence of galling during hot forming of Al-Si-coated high-strength steel. *Proceedings of the Institution of Mechanical Engineers, Part J: J Eng Tribol* 225:487–498. <https://doi.org/10.1177/1350650111398313>
13. Podgornik B, Jerina J (2012) Surface topography effect on galling resistance of coated and uncoated tool steel. *Surf Coat*

- Technol 206:2792–2800. <https://doi.org/10.1016/j.surfcoat.2011.11.041>
14. Kang Z, Fu Y, Chen Y, et al (2018) Experimental Investigation of Concave and Convex Micro-Textures for Improving Anti-Adhesion Property of Cutting Tool in Dry Finish Cutting. *Int J of Precis Eng and Manuf-Green Tech* 5:583–591. <https://doi.org/10.1007/s40684-018-0060-3>
 15. Zheng K, Politis DJ, Lin J, Dean TA (2017) An experimental and numerical investigation of the effect of macrot textured tool surfaces in hot stamping. *Int J Mater Form* 10:241–254. <https://doi.org/10.1007/s12289-015-1273-4>
 16. Cao Y, Hu R, Shi W, et al (2023) Experimental study on laser peen texturing and tribological properties of E690 high-strength steel. *Opt Laser Technol* 157:108784. <https://doi.org/10.1016/j.optlastec.2022.108784>
 17. Decrozant-Triquenaux J, Pelcastre L, Courbon C, et al (2021) Effect of surface engineered tool steel and lubrication on aluminium transfer at high temperature. *Wear* 477:203879. <https://doi.org/10.1016/j.wear.2021.203879>
 18. Hernandez S, Hardell, Jens, Prakash, Braham (2018) High-Temperature Friction and Wear of Boron Steel and Tool Steel in Open and Closed Tribosystems. <https://www.tandfonline.com/doi/epdf/10.1080/10402004.2017.1350310?needAccess=true>. Accessed 22 May 2024
 19. Mozgovoy S, Alik L, Hardell J, Prakash B (2019) Material transfer during high temperature sliding of Al-Si coated 22MnB5 steel against PVD coatings with and without aluminium. *Wear* 426–427:401–411. <https://doi.org/10.1016/j.wear.2018.12.042>
 20. Pelcastre L, Kurnia E, Hardell J, et al (2021) High temperature tribological studies on hardfaced tool steels for press hardening of Al-Si coated boron steel. *Wear* 476:203728. <https://doi.org/10.1016/j.wear.2021.203728>
 21. Wang Y, Ding Y, Jiang Y, et al (2022) The Effects of Die Temperature and Cooling Condition on Friction Behavior of Bare 22MnB5 Boron Steel in Hot Stamping. *Tribol Trans* 65:519–530. <https://doi.org/10.1080/10402004.2022.2040673>
 22. Yanagida A, Kurihara T, Azushima A (2010) Development of tribo-simulator for hot stamping. *J Mater Process Technol* 210:456–460. <https://doi.org/10.1016/j.jmatprotec.2009.10.007>

Publisher's Note Springer Nature remains neutral with regard to jurisdictional claims in published maps and institutional affiliations.

Springer Nature or its licensor (e.g. a society or other partner) holds exclusive rights to this article under a publishing agreement with the author(s) or other rightsholder(s); author self-archiving of the accepted manuscript version of this article is solely governed by the terms of such publishing agreement and applicable law.